EURASIP Journal on Applied Signal Processing 2005:1, 12–19

Symbol and Bit Error Rates Analysis of Hybrid PIM-CDMA

Z. Ghassemlooy
Optical Communications Research Group, School of Engineering & Technology, Northumbria University, Newcastle NE1 8ST, UK
Email: fary.ghassemlooy@unn.ac.uk

C. K. See
Optical Communications Research Group, School of Engineering & Technology, Northumbria University, Newcastle NE1 8ST, UK
Email: cksee1976@yahoo.com

Received 7 April 2004; Revised 17 August 2004

A hybrid pulse interval modulation code-division multiple-access (hPIM-CDMA) scheme employing the strict optical orthogonal code (SOCC) with unity and auto- and cross-correlation constraints for indoor optical wireless communications is proposed. In this paper, we analyse the symbol error rate (SER) and bit error rate (BER) of hPIM-CDMA. In the analysis, we consider multiple access interference (MAI), self-interference, and the hybrid nature of the hPIM-CDMA signal detection, which is based on the matched filter (MF). It is shown that the BER/SER performance can only be evaluated if the bit resolution M conforms to the condition set by the number of consecutive false alarm pulses that might occur and be detected, so that one symbol being divided into two is unlikely to occur. Otherwise, the probability of SER and BER becomes extremely high and indeterminable. We show that for a large number of users, the BER improves when increasing the code weight w. The results presented are compared with other modulation schemes.

Keywords and phrases: optical wireless, digital modulation, error rate, pulse modulation.

1. INTRODUCTION

As in RF wireless systems, diffuse optical wireless systems can employ a multiple access scheme for channel reuse strategy. The direct-sequence (DS-) CDMA is one promising scheme, which operates in both time and wavelength (frequency) domains, and can enhance the channel capacity when the wavelength resources are constrained. However this is achieved at the cost of reduced data throughput. A DS-CDMA system employing on and off keying (OOK), which is known as OOK-CDMA, utilises OOCs to form a signature signal for the purpose of message separation, thus enabling the transmission of a large number of asynchronous users. In DS-CDMA, encoding is carried out by "spreading" individual bits to form a signature sequence with a higher bandwidth. However, the bandwidth of a diffuse optical wireless system is limited by characteristics of the channel. Under such a bandwidth constraint, a DS-CDMA system's throughput is reduced, which is inversely proportional to the length of the signature sequence. It has been reported that OOK-CDMA offers advantages over OOK with an increased number of channels, but at the cost of reduced data throughput under limited bandwidth [1]. To improve system's power efficiency and the throughput without the need for bandwidth expansion and to enhance the data rates, hybrid pulse position modulation (hPPM)-CDMA system has been proposed [2, 3, 4]. However, system throughput can be further increased without the need for bandwidth expansion by employing hPIM-CDMA, which utilises a shorter symbol length to convey the same information as in hPPM-CDMA [5]. hPIM-CDMA system also offers much simpler design and implementation since the signal is anisochronous in nature and hence requires no symbol synchronisation when compared with the OOK-CDMA and hPPM-CDMA schemes [5]. Both hPIM-CDMA and hPPM-CDMA schemes achieve data compression by generating a shorter symbol length than OOK-CDMA. However, symbols with shorter lengths will have an effect on the error rate performance and the power efficiency as the signal power per symbol is being condensed. Moreover, the total signal power allowed to transmit is limited by the eye safety regulations. Thus these criterions impose new challenges to the system designers that need addressing.

However, by employing OCCS and good correlation properties the hPIM-CDMA performance can be improved.

In this paper, the error analysis of hPIM-CDMA system employing $(n, w, 1, 1)$ SOOC with the length n, code weight w, and unity auto- and cross-correlation constraints λ_a and λ_c, respectively, is presented. Minimum values of λ_c and λ_a are used to improve the error performance. For the first time the case where more than one symbol is in error due to false alarm is investigated, and the conditions for consecutive false alarm pulses occurring is also defined. The analysis takes into account the multiple access interference (MAI), the self-interference, and the hybrid nature of the hPIM-CDMA signal detection. In hPIM-CDMA employing $(n, w, 1, 1)$ SOOC, the distribution of MAI and self-interference are found to be binomial, whereas employing $(n, w, 1, 1)$ OOC, the distribution is multinomial. It shown that the BER performance can be evaluated if the values of bit mapping (M) conform to the condition set by the number of consecutive false alarm pulses that can be detected. Therefore, the possibility of one symbol being divided into two is unlikely to occur. Otherwise the probability of BER is indeterminable and high. The remaining of the paper is organised as follows. Section 2 will describe the theory of H-PIM-CDMA. The error analysis and results will be also discussed in Section 3, followed by concluding remarks in Section 4.

2. SYSTEM MODEL

Similar to the PIM, hPIM-CDMA offers improved throughput performance, which is measured by the normalised bit rate enhancement factor defined as $\mathrm{BEF}_{\mathrm{h\,PIM\text{-}CDMA/\,OOK}} = 2^M/(2n + 2^M - 1)$. This improvement achieved by eliminating the redundant chips as in hPPM-CDMA symbol [5]. The symbol is composed of a signature sequence followed by $S_k^i T_c$ empty chips given as $T_S = (n + S_k^i)T_c$. A system block diagram and typical waveforms for hPIM-CDMA are shown in Figure 1. The information bits $B_{k|\mathrm{Tx}}^i \in \{0, 1\}$ from the ith data source are first converted into PIM sequences before being fed into the tap-delay line (TDL) encoder. In carrying out the analysis, a number of assumptions were made, for example, (i) the chip is synchronous between transmitters and receivers, (ii) the dominant interferences are due to the self-interference and the uncorrelated signal better known as MAI, and the Gaussian noise, which is considered to be negligible, (iii) the near-far effect is not taken into account, (iv) the channel response is considered to be ideal for the normalised delay spread $D_T \leq 0.3$, and (v) the channel optical gain, the encoder peak output voltage, and the photodetector responsivity are all equal to unity.

An optical DS-CDMA is normally classified as a noncoherent system, where signature encoding is performed by an optical waveguide structure [6, 7]. However, in optical wireless diffuse systems, signature encoding and decoding can only be implemented in the electrical domain. Here conventional encoding and decoding techniques are employed at the transmitter and receiver. The encoder is composed of a parallel tap-delay structure, where each branch's delay value is determined by the codeword of the signature sequence. The encoded hPIM-CDMA signal that is nonperiodic is given as

$$d_{\mathrm{Tx}}^i(t - \tau_{d|\mathrm{Tx}}^i) = V_d \sum_{k=0}^{\infty} \sum_{j=1}^{w} g_c\left(t - cw_{(i,j)} - \left(nk + \sum_{l=-1}^{k-1} S_l^i\right) T_c - \tau_{d|\mathrm{Tx}}^i\right), \tag{1}$$

where k is the bit or symbol sequence number, I the number of users (channels), S_k^i the decimal value of the M-bit information, $\tau_{d|\,\mathrm{Tx}}^i$ the time delay of the ith transmitter, V_d the peak voltage of the encoder output signal, $g_c(t)$ the pulse sequence of duration T_c, and $cw_{(i,j)}$ the element of code word matrix.

At the receiver the detected signal d_{Rx}^i is passed through a matched filter (MF) detector. MF is composed of a TDL structure, with function opposite to that of the transmitter, where by tuning the delay values a higher amplitude signal pulse can be created by each of the pulses in the signature sequence. Tap-delay-based MFs provide high-speed rough synchronisation and offer more robust fine synchronisation over a wide range of dispersion compared with the correlator-based detectors. The decoded signal at the output of the TDL can be expressed as

$$\begin{aligned} e_{\mathrm{Rx}}^i(t) &= V_d R_{\mathrm{Rx}}^i \sum_{k=0}^{\infty} w g_c\left(t - (n-1)T_c - \left(nk + \sum_{l=-1}^{k-1} S_l^i\right) T_c - \tau_{d|\,\mathrm{Tx}}^i\right) \otimes h^{i|i}(t) \\ &+ V_d R_{\mathrm{Rx}}^i \sum_{k=0}^{\infty} \sum_{j=1}^{w} \sum_{J=1}^{w} g_c\left(t - cw_{(i,J)}T_c - (n-1-cw_{(i,j)})T_c - \left(nk + \sum_{l=-1}^{k-1} S_l^i\right) T_c - \tau_{d|\mathrm{Tx}}^i\right) \otimes h^{i|i}(t) \\ &+ R_{\mathrm{Rx}}^i \sum_{j=1}^{w} \sum_{I=1}^{F} D_{\mathrm{Tx}}^I\left(t - (n-1-cw_{(i,j)})T_c - \tau_{d|\,\mathrm{Tx}}^I\right) \otimes h^{I|i}(t) + n(t). \end{aligned} \tag{2}$$

Substituting (1) into (2) and considering the assumptions made above, the decoded signal can be written as

$$\begin{aligned} e_{\mathrm{Rx}}^i(t) = &\sum_{k=0}^{\infty} w g_c\left(t - (n-1)T_c - \left(nk + \sum_{l=-1}^{k-1} S_l^i\right) T_c - \tau_{d|\,\mathrm{Tx}}^i\right) \\ &+ \sum_{k=0}^{\infty} \sum_{j=1}^{w} \sum_{J=1}^{w} g_c\left(t - cw_{(i,J)}T_c - (n-1-cw_{(i,j)})T_c - \left(nk + \sum_{l=-1}^{k-1} S_l^i\right) T_c - \tau_{d|\,\mathrm{Tx}}^i\right) \\ &+ \sum_{k=0}^{\infty} \sum_{j=1}^{w} \sum_{J'=1}^{w} \sum_{I=1}^{F} g_c\left(t - cw_{(I,J')}T_c - (n-1-cw_{(i,j)})T_c - \left(nk + \sum_{l=-1}^{k-1} S_l^I\right) T_c - \tau_{d|\,\mathrm{Tx}}^I\right), \end{aligned} \tag{3}$$

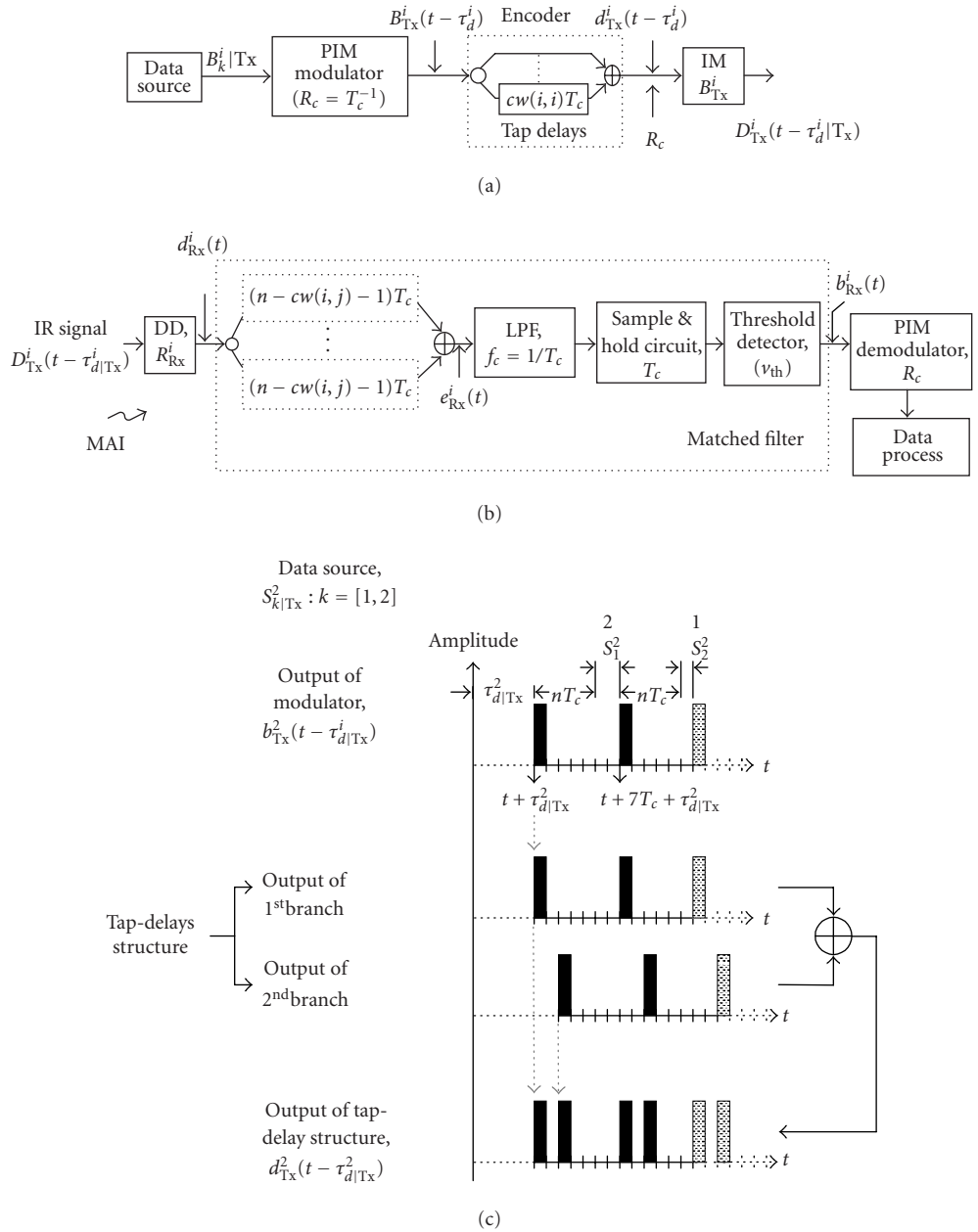

Figure 1: hPIM-CDMA: (a) transmitter block diagram, (b) receiver block diagram, and (c) timing waveforms.

where $i \neq I$ and $j \neq J$, $D^I_{\text{Tx}}(t-\tau^I_{d|\text{Tx}}) = d^I_{\text{Tx}}(t-\tau^I_{d|\text{Tx}})$. The 1st and 2nd terms are the decoded hPIM signal (or the auto-correlated peaks) and the autocorrelation constraints, respectively. The 3rd and 4th terms are the MAI and the Gaussian noise. Note the delayed (by $(n-1)T_c$) decoded signal in the 1st term due to the tap-delay structure.

The hPIM signal at the output of the MF assuming no MAI and Gaussian noise is given as

$$b^i_{\text{Rx}}(t) = V_T R^i_{\text{Tx}} R^i_{\text{Rx}} \sum_{k=0}^{\infty} g_c\left(t - \left(k + \sum_{l=-1}^{k-1} S^i_l\right) T_c - \tau^i_{d|\text{Tx}}\right), \tag{4}$$

where V_T is the peak voltage of the threshold detector output, for other notations see Figure 1. Finally, the data is recovered by employing a standard PIM demodulator as in [8] with minor modifications. Since hPIM symbol contains extra $(n-1)$ chips (redundancy resulting from CDMA decoding), then when the demodulator detects a pulse of $1T_c$ duration at the start of a symbol, it ignores the following $(n-1)T_c$ chips; then count the number of empty chips of $S^i_k T_c$ that corresponds to the information [9].

The normalised BEF and power efficiency W_{Eff} of the hPIM-CDMA together with other modulation schemes are given in Table 1.

Table 1: The power efficiency and BEF expressions for various DS-CDMA schemes normalised to OOK. Note that $n = Fw(w-1)$ for optimal $(n, w, 1, 1)$ OOC.

System	W_{Eff}	BEF
OOK-CDMA/OOK	$-10\log_{10}(wF/n)$ (dB)	$1/n$
PPM-CDMA/OOK	$-10\log_{10}(2wF/n2^M)$ (dB)	$M/n2^M$
hPPM-CDMA/OOK	$-10\log_{10}[2wF/(2n+2^M-1)]$ (dB)	$M/(n+2^M-1)$
hPIM-CDMA/OOK	$-10\log_{10}[4wF/(2n+2^M-1)]$ (dB)	$2M/(2n+2^M-1)$

For hybrid schemes, power efficiency is highly dependent on the set of signature sequences and bit resolution M that one could use. The average transmitted power is low when employing optimum $(n, w, 1, 1)$ OOC of $w \geq 4$.

3. SYMBOL AND BIT ERROR RATES ANALYSIS AND RESULTS

Observing the second term in (4), there are $w-1$ pulses, represented by J, whose positions do not match with the w TDLs, represented by j. This produces $w(w-1)$ uncorrelated pulses of unity amplitude ($\lambda_a = 1$) at the output of the MF detector that will spread into two regions of duration $(n-1)/2$ chips alongside the signal pulse, see Figure 2.

From (4), the distance (rather than the delay) that the uncorrelated pulses will spread is $D_S = cw_{(i,J)} + (n-1-cw_{(i,j)})$. T_c is omitted here since it is irrelevant. The length where all $w(w-1)$ uncorrelated pulses are contained is $D_{L|S} = D_{S|\max} - D_{S|\min}$. $D_{S|\min}$ and $D_{S|\max}$ are determined by substituting $\min(cw_{(i,J)})$ and $\max(cw_{(i,j)})$, and $\max(cw_{(i,J)})$ and $\min(cw_{(i,j)})$ into D_S, respectively. From (3), S_k^i does have an effect on the distance of the $w(w-1)$ pulses with relation to the reference time t. Hence, the probability of self-interference from every symbol taken independently assuming independent, identical distributed S_k^i, is defined as

$$P_{\lambda_a|h\text{PIM-CDMA}} = \frac{w(w-1)}{D_{L|s} + S_k^i} = \frac{2w(w-1)}{2n+2^M-3}. \tag{5}$$

It is found that for all $(n, w, 1, 1)$ SOOC sets $D_{L|\text{Spread}} = n-1$. From the 3rd term in (3), each I has w pulses with positions not matched with the i desired user MF detector TDL values. Since there are w parallel TDLs of the i MF detector then the output produces w^2 uncorrelated pulses. Therefore the probability of interference due to MAI is given as

$$P_{\lambda_c} = \frac{2w^2}{2n+2^M-1}. \tag{6}$$

For MAI, $D_{L|\text{Spread}}$ is n, since none of the MAI signal pulses match the desired i codeword and hence all w^2 pulses are spread over the entire n chip region. Each interfering signal is transmitting at random, that is, $0 \leq \tau_{d|\text{Tx}}^i \bmod_{n+2^M-1} < (n+2^M-1)T_c$ where $\tau_{d|\text{Tx}}^i$ is an integer multiple of T_c. The time-delay limit is the worst case where all users are transmitting simultaneously. Each signal interfering with the desired signal at a single chip position displays a probability density function (PDF) given as

$$\text{PDF}(x) = (1-P_{\lambda_c})\delta(x) + P_{\lambda_c}\delta(x-1). \tag{7}$$

Therefore, the MAI effect on the desired signal at a single chip position will display a Binomial distribution B expressed as

$$\text{PDF}_{B\cdot\text{MAI}}(x) = \sum_{i=0}^{F-1} \binom{F-1}{i} (P_{\lambda_c})^i \cdot (1-P_{\lambda_c})^{F-1-i}\delta(x-i). \tag{8}$$

In hPIM-CDMA, demodulation is carried out by detecting a pulse at the start of a symbol, then ignoring $n-1$ chips and counting the number of empty chips γ until the next pulse is detected. In an error-free case, the next pulse detected is the beginning of the next symbol. However, due to false alarm, a new pulse could be generated within γ-slots that result in a symbol being in error. For F users transmitting simultaneously, each desired signal is interfered by $F-1$ other signals as well as self-interference. The probability of a false alarm pulse occurring in the γ-slots exceeding the threshold level v_{th} due to the self-interference and MAI is given as, first and second terms, respectively,

$$\begin{aligned} P_{fa} = {} & P_{\lambda_a} \sum_{i=v_{\text{th}}-1}^{F-1} \binom{F}{i+1} (P_{\lambda_c})^i \cdot (1-P_{\lambda_c})^{F-1-i} \\ & + (1-P_{\lambda_a}) \sum_{i=v_{\text{th}}}^{F-1} \binom{F}{i} (P_{\lambda_c})^i \cdot (1-P_{\lambda_c})^{F-1-i}. \end{aligned} \tag{9}$$

There are two conditions by which the error rate could be defined by means of symbol error rate (SER) and/or BER. First, a symbol cannot be divided into two, which will result in more than two symbols being in error. In PIM, a symbol in a packet due to a false alarm error will affect not only the next symbol in error but also the remaining symbols in the packet by changing their relative positions [5]. In such cases, the system error rate is determined by the packet error rate (PER) rather than SER or BER. In hPIM-CDMA, an error in a symbol only affects the next symbol but not the rest of the symbols. This is because the false alarm has been treated as the next symbol pulse and the pulse of the next symbol has been ignored. This will only result in the current and the next symbol lengths being shorter and longer, respectively.

A symbol is divided into two if the presence of a false alarm pulse does not result in deleting or missing the pulse of

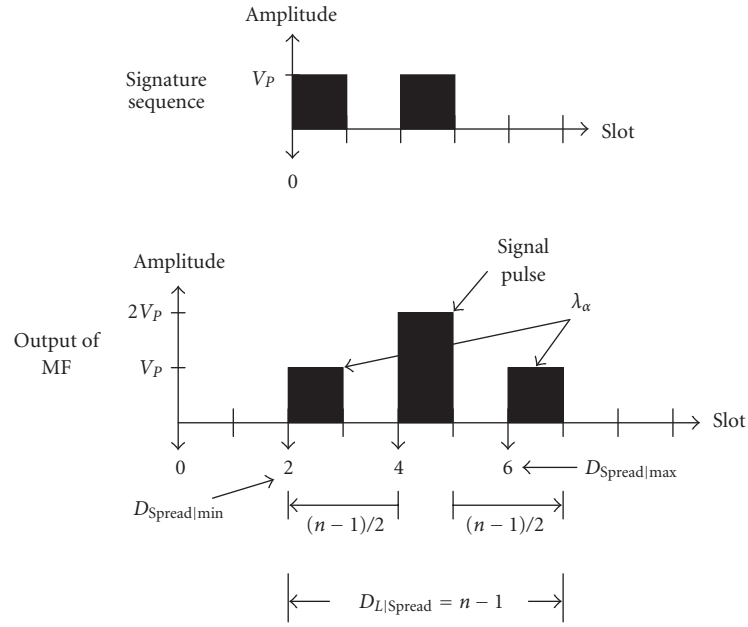

Figure 2: Autocorrelation constraints of $(5, 2, 1, 1)$ SOOC.

the next symbol. There are two cases in which this can occur. (1) The mapping order L is so large that $S_k^i > n$. When the demodulator detects a false alarm pulse within S_k^i, it cannot ignore the pulse of the next symbol when not considering the $n-1$ empty chips, see Figure 3a. (2) P_{SFA} is high such that $S_k^i \leq n$, and there is a high probability of a false alarm pulse occurring in every symbol, see Figure 3b. In this case, a false alarm pulse divides a symbol into two if the following holds:

$$\gamma_1 + n_2 + \gamma_2 + n_3 + \gamma_3 + 1 > n_{f|1} + \gamma_{f|1} + n_{f|2} + \gamma_{f|2} + n_{f|3}. \tag{10}$$

The limit of the condition, the worst case, is when γ's on the left-and right hand-sides are all maximum and equal to zero, respectively. Rewriting (10), the condition can be generalised as

$$\begin{aligned}(2^M-1)+n_2+(2^M-1)+n_3+(2^M-1)+1 &\leq n_{f|1}+n_{f|2}+n_{f|3},\\ 2^M-1 &\leq \frac{n-1}{3}.\end{aligned} \tag{11}$$

Note that all n's are equal. The division by 3 can easily be seen, as a factor from 3 consecutive false pulses that must occur one after another at a distance of $n-1$ chips away from each another. The condition for consecutive false alarm pulses to occur is given by

$$z_{\text{NS}} = \frac{n-1}{2^M-1}. \tag{12}$$

The probability that a new symbol will exist due to the worst case scenario where z_{NS} consecutive symbols are at maximum length, and z_{NS} consecutive false alarm pulses are occurring, is given by

$$P_{\text{NS}} = \left(\frac{P_{\text{CFA}}}{2^M}\right)^{z_{\text{NS}}}. \tag{13}$$

Using (12), the 5th plot of z_{NS} against F and M for $(n, 3, 1, 1)$ SOOC is shown in Figure 4a. This shows the lower bound for z_{NS} for $P_{\text{NS}} = 10^{-13}$. For $z_{\text{NS}} > 30$, the P_{NS} will reduce even further. The lower bound for z_{NS} is given as

$$z_{\text{NS}} \geq \left\lfloor \frac{Fw(w-1)}{2^M-1} \right\rfloor \geq 30. \tag{14}$$

Increasing w will reduce P_{NS} and z_{NS}, this is because the code weight that contributes to the autocorrelation peak magnitude will increase the signal-to-interference ratio.

The second condition is that no two or more false alarm pulses will occur in two or more consecutive symbols, respectively. When one or more false alarm pulse occurs, the length of the current and next symbols is shortened and lengthened, respectively. The cumulative probability of one or more false alarm pulses that can occur in each of two consecutives symbols is given as

$$P_{2\,\text{SFA}} = \frac{P_{\text{CFA}}^2}{2^{2M}} \sum_{\gamma_1=1}^{2^M-1} \gamma_1 \left(\left[\sum_{\gamma_2=\gamma_1}^{2^M-1+\gamma_1} \gamma_2 \right] - 2^M \right). \tag{15}$$

Hence, (14) is redefined according to the condition that if the cumulative probability exceeded one, that is more than one false alarm pulses have occurred, then two symbols are definitely in error and so $P_{2\,\text{SFA}}$ is set to 1. Else, $P_{2\,\text{SFA}}$ remains

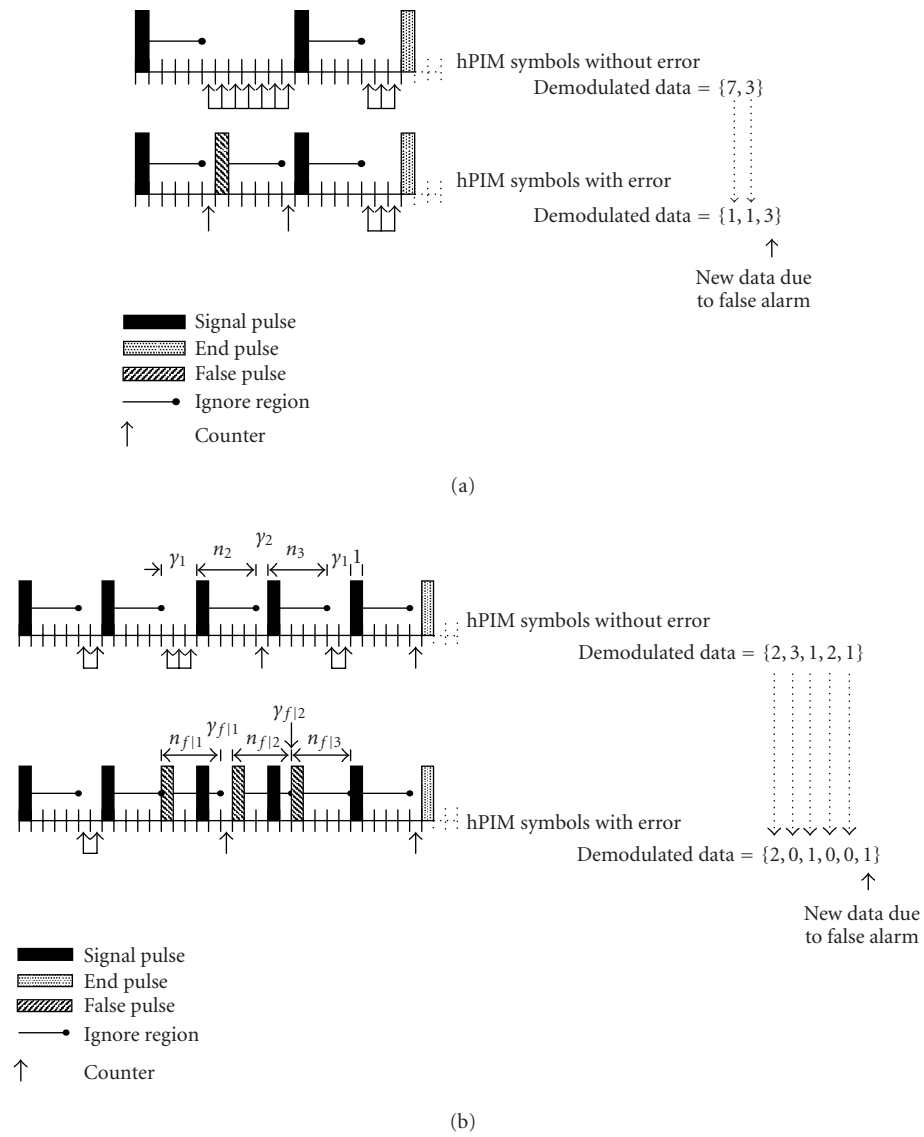

Figure 3: Illustration of the probability of a symbol being divided into two: (a) $n = 5$ and $M = 3$, and (b) $n = 5$ and $M = 2$.

unchanged that is defined as

$P_{2\,\mathrm{SFA}}$
= [(Probability of false alarm occurring in the current symbol) × (Probability of false alarm occurring in the next symbol) − (Probability of false alarm occurring in the current symbol) × (Probability of false alarm occurring in the next symbol at a position causing no error in the next symbol)],

$$P_{2\,\mathrm{SFA}} = \begin{cases} \left\{ \dfrac{P_{\mathrm{CFA}}^2}{2^{2M}} \displaystyle\sum_{\gamma_1=1}^{2^M-1} \gamma_1 \left(\left[\sum_{\gamma_2=\gamma_1}^{2^M-1+\gamma_1} \gamma_2 \right] - 2^M \right) \right\} & \text{if } \{\cdot\} < 1, \\ 1 & \text{if } \{\cdot\} \geq 1. \end{cases} \tag{16}$$

The SER can be approximated if the probability of two or more consecutive symbols being in error is assumed to be low compared with the probability of one symbol being in error. Knowing that the probability of three or more consecutives symbols being in error is lower than two consecutive symbols, then only the probability of one symbol and two consecutive symbols being in error are compared. Following (15), the probability of one symbol being error is expressed as

$$P_{1\,\mathrm{SFA}} = \begin{cases} \left[\dfrac{2^M - 1}{2} \right] P_{\mathrm{CFA}} & \text{if } \{\cdot\} < 1, \\ 1 & \text{if } \{\cdot\} \geq 1. \end{cases} \tag{17}$$

Using (16) and (17), the probabilities of one and two consecutive symbols being in error against F and w are shown in Figure 4b. As can be seen, the probability of one symbol

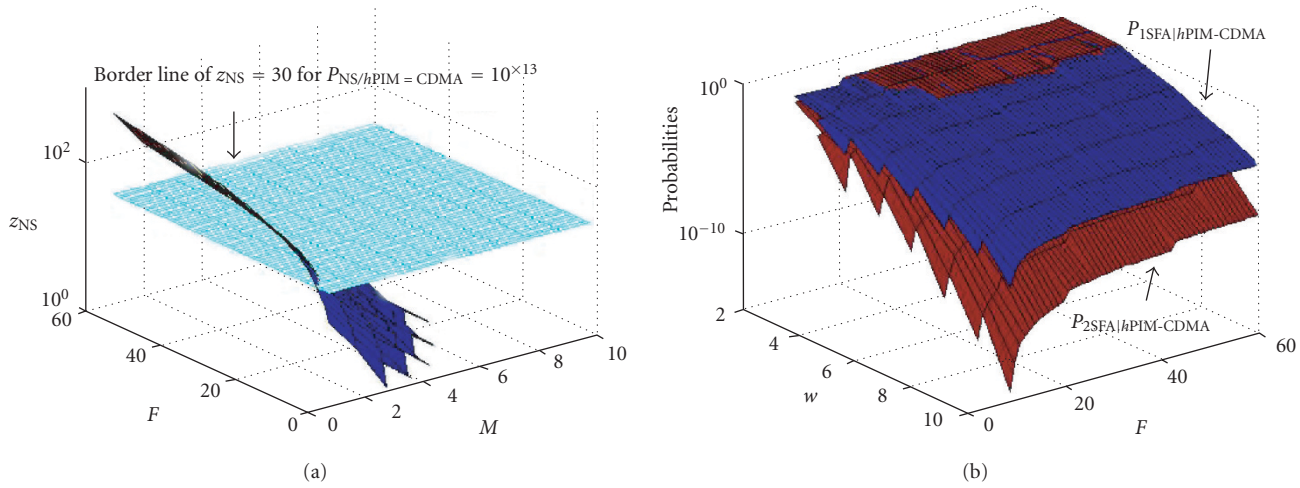

FIGURE 4: (a) z_{NS} against F and M for optimal $(n, 3, 1, 1)$ SOOC and (b) probabilities of one symbol and two consecutive symbols being in error against F and w.

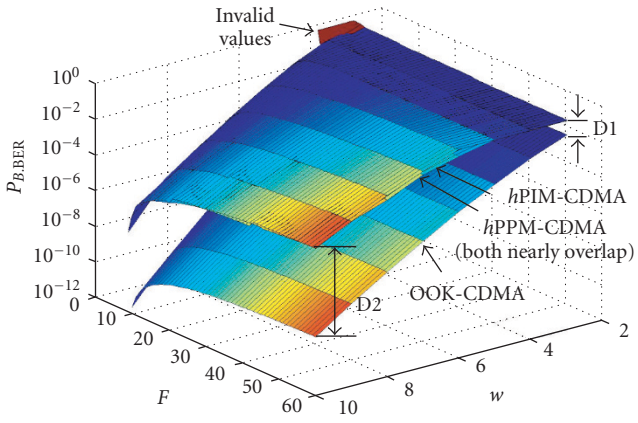

FIGURE 5: BER performance of OOK-CDMA, hPIM-CDMA, and hPPM-CDMA against F and w.

being in error is more likely to happen than the probability of two consecutive symbols being in error when $w > 5$. For $w \leq 5$ and $F > 20$, both probabilities are equal to one. Therefore, hPIM-CDMA SER can be approximated based on (17) alone. When one symbol is in error, then two symbols will be detected incorrectly, hence SER is given as

$$P_{SER} \approx \begin{cases} (2^M - 1)P_{CFA} & \text{if } \{\cdot\} < 1, \\ 1 & \text{if } \{\cdot\} \geq 1. \end{cases} \quad (18)$$

Conversion from SER to BER can be carried out using $P_{BER} = [2^M/2(2^M - 1)]P_{SER}$ [10]. Figure 5 shows the BER performance against F and w for hPIM-CDMA. Also shown for comparison are results for OOK-CMD and hPPM-CDMA. The value of M for each value of F and w is obtained from (14). As shown in Figure 4 hybrid schemes display similar BER performance compared with OOK-CDMA. The BER decreases linearly and increases nonlinearly with w and F, respectively. For both hybrid schemes BER ≥ 0.5 for $w = [3, 4]$ and all values of F, and for $w = 5$ and $F \geq 25$. This is due to the severity of the MAI, which results in an SER ≈ 1. Note that SER of 1 does not correspond to a BER of 1. In hybrid schemes, a symbol maps to M number of bits, thus when one symbol is in error only some bits will be in error. Hence, for all possible symbols, the average number of bits being in error is determined by P_{BER}, which is a function of M. For $w > 5$, the BER for both hybrid schemes decreases linearly, this is because the code weight that contributes to the autocorrelation peak magnitude will increase the signal-to-interference ratio, thus resulting in reduce P_{NS} and z_{NS}. For hPIM-CDMA, the BER is forced to 1 for small values of F and w as indicated by the "invalid values." This is because these values do not satisfy the condition in (14). Notice the difference between the hybrid and OOK-CDMA schemes, indicated by D1 and D2. This is because as w increases from 3 to 10, M increases from 3 to 7. Referring to (18), increasing M will increase the average length of the information slots (i.e., $2^M - 1$) of hPIM-CDMA symbol, which will result in increased P_{CFA}.

4. CONCLUSIONS

In this paper, comprehensive error analyses for hPIM-CDMA employing $(n, w, 1, 1)$ SOOC, an MF detector with a TDL structure and taking into account MAI, self-interference was presented. It was shown that SER and BER could only be evaluated if the values of bit mapping M conform to the condition set by the number of consecutive false alarm pulses that might be detected. Therefore, the possibility one symbol being divided into two is unlikely to occur. Otherwise the probability of BER is indeterminable and high. We have shown that hPIM-CDMA BER performance is similar to hPPM-CDMA, and is highly dependent on the code weight w, F, and M.

REFERENCES

[1] R. Matsuo, M. Matsuo, T. Ohtsuki, T. Udagawa, and I. Sasase, "Performance analysis of indoor infrared wireless systems using OOK CDMA on diffuse channels," in *Proc. IEEE Pacific Rim Conference on Communications, Computers and signal Processing (PACRIM '03)*, pp. 30–33, Victoria, British Columbia, Canada, August 1999.

[2] J. M. H. Elmirghani and R. A. Cryan, "Indoor infrared wireless networks utilising PPM CDMA," in *Singapore ICCS Conference Proceedings*, vol. 1, pp. 334–337, Singapore, November 1994.

[3] O. Tomoaki, S. Iwao, and M. Shinsaku, "Effects of hard-limiter and error correction coding on performance of direct-detection optical CDMA systems with PPM signalling," *IEICE Trans. Fundamentals*, vol. E78-A, no. 9, pp. 1092–1101, 1995.

[4] S. S. Hwang, C. Park, and J. H. Lee, "Asynchronous multi-rate optical wireless PPM-CDMA in an indoor non-directed diffuse channel," *Electronics Letters*, vol. 33, no. 18, pp. 1565–1567, 1997.

[5] C. K. See, Z. Ghassemlooy, and J. M. Holding, "Hybrid PIM-CDMA for optical wireless networks," in *Proc. 1st Annual PostGraduate Symp. on the Convergence of Telecommunications, Networking and Broadcasting (PGNET '00)*, pp. 195–200, Liverpool, UK, June 2000.

[6] J. Oksa, "S-38.220 licentiate course on signal processing in communications, FALL - 97 Optical CDMA systems," preprint, 1997, http://keskus.hut.fi/opetus/s38220/reports_97.

[7] J. Y. Hui, "Pattern code modulation and optical decoding—a novel code-division multiplexing technique for multifiber networks," *IEEE J. Select. Areas Commun.*, vol. 3, no. 6, pp. 916–927, 1985.

[8] Z. Ghassemlooy, N. L. Hayes, A. R. Seed, and E. D. Kaluarachchi, "Digital pulse interval modulation for optical communications," *IEEE Commun. Mag.*, vol. 36, no. 12, pp. 95–99, 1998.

[9] A. R. Hayes, *Digital pulse interval modulation for indoor optical wireless communication systems*, Ph.D. thesis, Sheffield Hallam University, Sheffield, UK, 2002.

[10] J. G. Proakis, *Digital Communications*, McGraw-Hill, New York, NY, USA, 3rd edition, 1995.

Z. Ghassemlooy received his B.S. (with honors) degree in electrical and electronics engineering from Manchester Metropolitan University in 1981, and the M.S. and Ph.D. degrees from the UMIST, UK, in 1984 and 1987, respectively. In 1988, he joined the City University, London, as a Research Fellow, and then moved to Sheffield Hallam University as a Lecturer, where he became a Professor in 1997. In 2004, he joined the School of Engineering and Technology, Northumbria University, Newcastle, UK, as an Associate Dean for research. In 2001, he was a recipient of the T. C. Tuan Fellowship in Engineering from the Nanyang Technological University, Singapore. He is the Editor-in-Chief of the Mediterranean Journal of Electronics and Communications and the Mediterranean Journal of Computers and Networks, and serves on the Editorial Boards of the International Journal of Communication Systems, the Sensor Letters, and EURASIP Journal on Wireless Communications and Networking. He is the Founder and Chairman of the International Symposium on Communication Systems, Network and DSP, and is a Technical Committee Member of a number of international conferences. He has published over 200 papers and is a Co/Guest-Editor of a book and a number of journals. His research interests are in photonic networks, modulation techniques, optical wireless, and optical fibre sensors. He is a Fellow of the IEE and a Senior Member of IEEE, and is currently the IEEE UK/IR Communications Chapter Secretary.

C. K. See graduated with a B.Eng. (with honors) degree in electronic systems and information engineering and a Ph.D. degree from Sheffield Hallam University in 1998 and 2003, respectively. He joined ActiveMedia Innovation Sdn. Bhd., Malaysia, in 2004 as a Technical Specialist. His main duties include delivering technical training courses using Matlab and Simulink. His research interests are in RF wireless communication systems, control systems, and chemical engineering. He is a Member of the IEEE.